ACS APPLIED MATERIALS & INTERFACES

Research Article

www.acsami.org

Aligned SWNT Films from Low-Yield Stress Gels and Their Transparent Electrode Performance

Ranulfo Allen, Gerald G. Fuller,* and Zhenan Bao*

Department of Chemical Engineering, Stanford University, Stanford, California 94305-5025, United States

Supporting Information

ABSTRACT: Carbon nanotube films are promising for transparent electrodes for solar cells and displays. Large-area alignment of the nanotubes in these films is needed to minimize the sheet resistance. We present a novel coating method to coat high-density, aligned nanotubes over large areas. Carbon nanotube gel dispersions used in this study have aligned domains and a low yield stress. A simple shearing force allows these domains to uniformly align. We use this to correlate the transparent electrode performance of single-walled carbon nanotube films with the level of partial alignment. We have found that the transparent electrode performance improves with increasing levels of alignment and in a manner slightly better than what has been previously predicted.

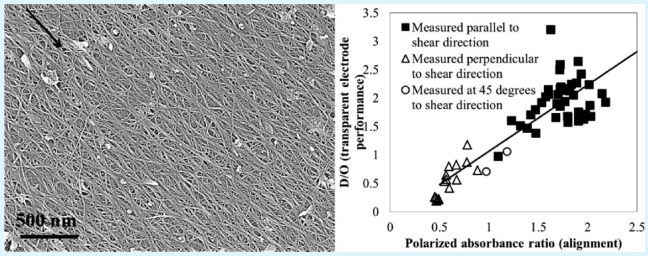

KEYWORDS: *carbon nanotube alignment, transparent electrodes, carbon nanotube thin films, solution processing, thin film coating*

Because of their unique electronic properties,[1] single-walled carbon nanotubes (SWNTs) are attractive for applications in the electronics industry. SWNTs have great potential as transparent electrodes, electrodes in organic electronics, transistors, or supercapacitors.[2−12] However, one major challenge is the electrical resistance that is observed in SWNT network films despite the extraordinary electrical conductivity of single SWNTs. This resistance is mainly attributed to the resistance occurring at tube−tube junctions.[3] One proposed method is to reduce the density of junctions in a film. This can be achieved by either using longer nanotubes[13−15] or aligned nanotubes.[16] Simulations have shown that partial alignment can indeed reduce the resistivity compared to a randomly oriented film.[16,17] However, this has not been demonstrated experimentally because of the lack of a controllable method that can achieve tunable alignment while maintaining a high tube density. There have been many studies attempting to align CNTs.[4,18−42] These studies have used methods such as utilizing chemical vapor deposition (CVD),[19−25] embedding CNTs in liquid crystals,[26−28] spin-coating,[4] and using concentration dependent self-alignment.[39−44] However, none of these methods are ideal. Some are too costly and/or have a low throughput, whereas others are not scalable or have poor density control. A new alignment method is introduced here that is easily scalable to large areas and is compatible with different substrates. Though further improvements are still needed, it suggests a promising processing strategy to align SWNTs.

This method involves forming aligned SWNT domains in solution, similar to a lyotropic liquid crystal. However, these dispersions are aligned gels with very low yield stresses on the order of a few pascals.[45] Thus, low stresses can be used to uniformly align a SWNT film. The gels are formed using a conjugated polymer, regioregular poly (3-hexylthiophene) (P3HT) as a dispersant for single-walled carbon nanotubes (SWNTs).[46] The P3HT wraps around the SWNTs.[47,48] In chlorinated, aromatic solvents, such as 1, 2-dichlorobenzene (oDCB), the polymer interacts with multiple SWNTs to form an interconnected network, which is the basis for gel formation.[45] A simple shearing force can subsequently align the SWNTs. The level of alignment can be systematically varied using this method. These dispersions are unique in that higher concentrations are typically needed to form ordered domains in solution and therefore allows the possibility of forming a high-density, aligned SWNT film. Other systems have also used moisture-sensitive superacids or insulating DNA to form these domains. Polythiophene is semiconductive, making it more suitable for electronic device applications.

A variety of deposition methods can yield films with different levels of partial alignment. By using a simple shearing blade with a birefringent, gelated SWNT dispersion, the alignment and density of the SWNT film could be modified by changing the shearing speed, gap, or dilution. This solution-processable deposition method is also attractive because of its low cost and scalability. It is important to note that the degree of alignment is not as high as in aligned, CVD-grown nanotubes. Instead, partial alignment is achieved. However, previous studies have predicted that perfect alignment is not ideal for conduction in nanotube films.[16,17,25,49]

Received: April 29, 2013
Accepted: July 3, 2013
Published: July 3, 2013

In addition, the effect of alignment on device performance will be discussed. Because various levels of alignment can be achieved, a correlation between alignment and performance can be obtained. Rogers et al. have attempted to use transistor performance for this correlation.[25,49] However, with their alignment method by CVD growth, the morphology of the nanotubes varied with levels of CNT density, alignment, and tube length, which the authors acknowledge. CNT density and tube length have a great impact on transistor performance. Since alignment could not be varied independent of other parameters, only limited conclusions could be made. For these reasons, transparent electrode performance will be measured in this study. The film transmittance and the sheet resistance are measured. The film transmittance also tracks the CNT density quantitatively. The changes in alignment should lead to changes in the sheet resistance. This will allow us to keep the CNT density constant by having the same transmittance while characterizing the dependence of sheet resistance on alignment. This study will probe the effective improvement in performance with increasing alignment and compare this with previously published simulation results.[16,17]

MATERIALS AND METHODS

Arc-discharged single-walled carbon nanotubes (ASP-100F) were purchased from the Hanwha Nanotech Corp, Korea. The nanotubes have an average diameter of about 1.4 nm. All other materials were purchased from Sigma-Aldrich (US) and used as received unless otherwise stated. Regioregular poly (3-hexyl thiophene) (P3HT) was used to disperse and align the nanotubes. No further purification of the materials was carried out. The composite dispersions were made by adding the appropriate amounts of polymer and SWNT into a small vial so as to have a 1:1 or 2:1 weight ratio. 1,2-Dichlorobenzene (oDCB) was then added to make a SWNT dispersion (2 mg SWNT/mL). The dispersion was then sonicated using a Cole-Palmer Ultrasonicator at 300 W for 15 min in an ice bath. After sonication at the above conditions, the SWNT length is about 1.5 μm. Note that no further centrifugation or purification was carried out after sonication.

Films were made using a motorized film applicator with a Mayer rod, Baker, or a Bird attachment (Elcometer, UK). The gap was varied between 10 and 40 μm. The films were cast at varying speeds from 4 μm/s to 100 mm/s. The solvent was then evaporated at room temperature to create the thin films. Some films were cast onto substrates heated up to 100 °C. All depositions were done within hours of the sonication. The polymer was removed by heating the films up to 500 °C for 1 h under an argon flow. All data and images represent films with the polymer removed unless stated otherwise. The resulting SWNT films were imaged using a FEI XL30 Sirion Scanning Electron Microscope (SEM). A thin layer of gold was sputtered onto the films for the SEM imaging. The alignment and transmittance were probed using a Cary 6000i UV−vis−NIR spectrophotometer. Using a polarizer and varying its polarization axis allows for observing differences in absorption due to alignment of the film. A four point probe with 5 mm spacing was used to measure sheet resistance. Samples were cut into 10 mm × 30 mm rectangles for the measurement and the geometry was taken into account for calculation of the sheet resistance.

RESULTS AND DISCUSSION

Our SWNT/P3HT dispersions, at a 1:1 or 2:1 weight ratio, form gels that contain aligned domains similar to liquid crystal solutions.[45] 1:1 and 2:1 dispersions have very similar rheological properties with 1:1 dispersions having more excess polymer, which leads to a slightly greater gel-like quality.[45] The degree of alignment is similar for both weight ratios. To demonstrate the alignment, we placed a drop of dispersion between crossed polarizers. Images were taken every 10 s as the drop dried. The beginning and end images are shown in Figure 1 and the entire video is available as Supporting Information.

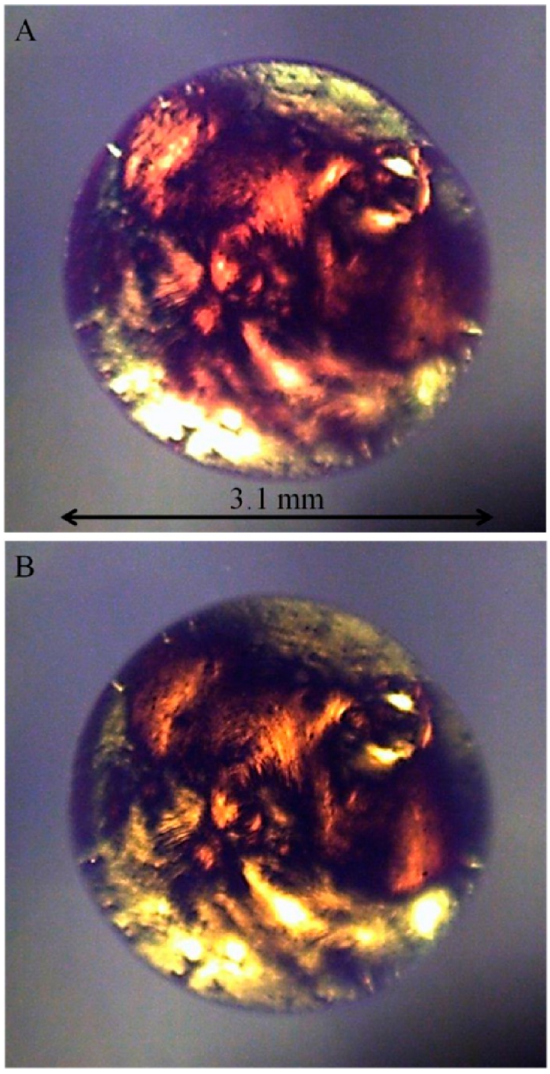

Figure 1. Evaporation of a drop of a SWNT/P3HT (1:1) in 1, 2-dichlorobenzene placed between crossed polarizers. Different light intensities represent different aligned domains. (A) Before evaporation. (B) After evaporation as a dried film.

The areas of different light intensity represent aligned domains of different orientations. This texture is similar to those typical for nematic liquid crystals when placed between crossed polarizers. It is important to note that the orientations of the domains do not change during the evaporation. This is due to the gel-like properties of the material.[45] There is minimal flow and thus minimal alignment changes. However, under a shear force, the domains can be aligned, similar to liquid crystals and this will be utilized to prepare aligned films. The detailed rheological behavior of these gels has been reported previously.[45]

SWNT films were made by using the above SWNT/P3HT dispersions. These dispersions were deposited onto glass slides using a modified automated film applicator (Elcometer 4340). The solvent was then allowed to dry. For heated samples, the applicator table was uniformly heated prior to the deposition using an attached, large, silicone rubber, etched-foil heater

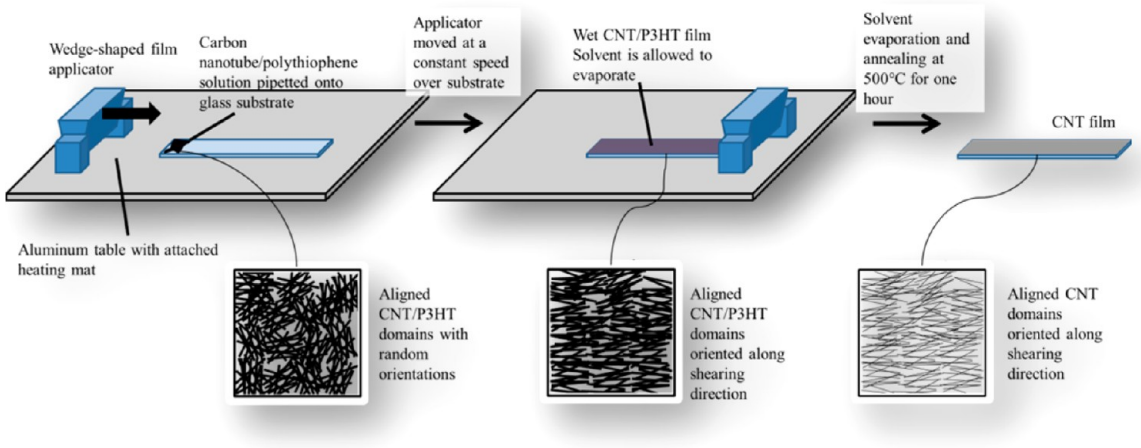

Figure 2. Cartoon demonstrating the procedure to make aligned carbon nanotube films.

(Omega Engineering). This process is demonstrated in Figure 2. To probe the range of alignment, we varied three conditions: the shear rate, the geometry of the film applicator, and the substrate temperature.

To determine the degree of alignment, we deposited films at various shear rates. Here, the shear rate is defined by the velocity of the moving head divided by the gap. The shear rate ranged from of 0.1 to 5000 s^{-1}. The alignment may not necessarily improve with increasing shear rate because the material is a shear thinning fluid.[45] After films were made using appropriate shear rates, the polymer was removed by placing them in a 500 °C furnace for one hour under an argon flow. Polarized absorption of the films was performed where the absorption of light polarized parallel and perpendicular to the shearing direction were measured. The ratio of the two can be used as a qualitative parameter to describe the level of SWNT alignment in the films.[26,50,51]

The data in Figure 3 are presented as the ratio of absorption of light polarized parallel to the shearing direction to absorption

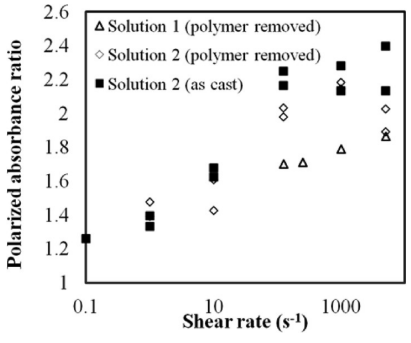

Figure 3. Effects of shear rate. Polarized absorbance ratios of SWNT/P3HT films at a 1:1 weight ratio for two batches cast at room temperature. Values are given for absorption at 1000 nm. Only SWNTs absorb at this wavelength. The applied shear rate was varied to yield a range of polarized absorbance ratio values.

of light polarized perpendicular to the shearing direction at the SWNT S_{11} absorption peak (1000 nm), at which P3HT does not absorb. Therefore, any dichroism due to the P3HT is avoided and the ratio of absorption characterizes only the alignment of the SWNTs. The polarized absorbance ratios are shown as a function of shear rate. Three data sets are presented: two are of the same films before and after the polymer removal, and the other is of films cast from a second dispersion. These data represent films made with the substrate at room temperature. The maximum polarized absorbance ratio obtained is 2.4. This is comparable to other reported alignment methods such as using vertically aligned CVD-grown nanotubes,[19] embedding CNTs into liquid crystals,[26] and a compression-sliding method.[35] In Figure 3, there is also some variability between the two batches. To be consistent, the same dispersion batch was used for most of the results. As shown, the ratio is dependent on the shear rate. However, there is very little change above 125 s^{-1}. It appears the level of alignment plateaus above this shear rate. It is also interesting to note that at shear rates as low as 0.1 s^{-1}, the polarization ratio is already greater than 1. Even at such a low shear rate, there is still some partial alignment. Dropcast films have also been made. Without an applied shear, these films are randomly oriented, with a polarized absorbance ratio of 1.0. In Figure 3, there is also a slight drop in the polarization ratio after polymer removal especially at larger shear rates. This indicates that the heat treatment does have a small adverse effect on the alignment. This is further demonstrated in images A and B in Figure 4, which show SEM images of a film before and after polymer removal. The black arrows represent the shearing direction. The nanotubes are curved and not as straight after the polymer removal and this curvilinearity may have caused the decrease of the degree of alignment found in other samples. Images C and D in Figure 4 show SEM images of films of lower alignment. Films with a low overall alignment contain some aligned domains that do not match the shearing direction. For all samples, the diameters of the SWNT bundles ranged from 10 to 30 nm after polymer removal.

Modifying the deposition temperatures varies the solvent evaporation rate and allows one to determine if the observed alignment plateau can be attributed to the solvent evaporation step. As the solvent slowly evaporates, the nanotubes could potentially lose the alignment gained from the shearing. As discussed, with the drop drying, there is minimal flow during the evaporation but this small amount of flow could still disrupt the alignment. Films were made at 25, 50, 75, and 100 °C. Figure 5A shows the polarized absorbance ratio for these films. All four films have a similar absorbance ratio; however, the films cast at lower temperatures have the greatest alignment. This shows that the nanotubes do not fluctuate much during the evaporation at room temperature, which would have disturbed

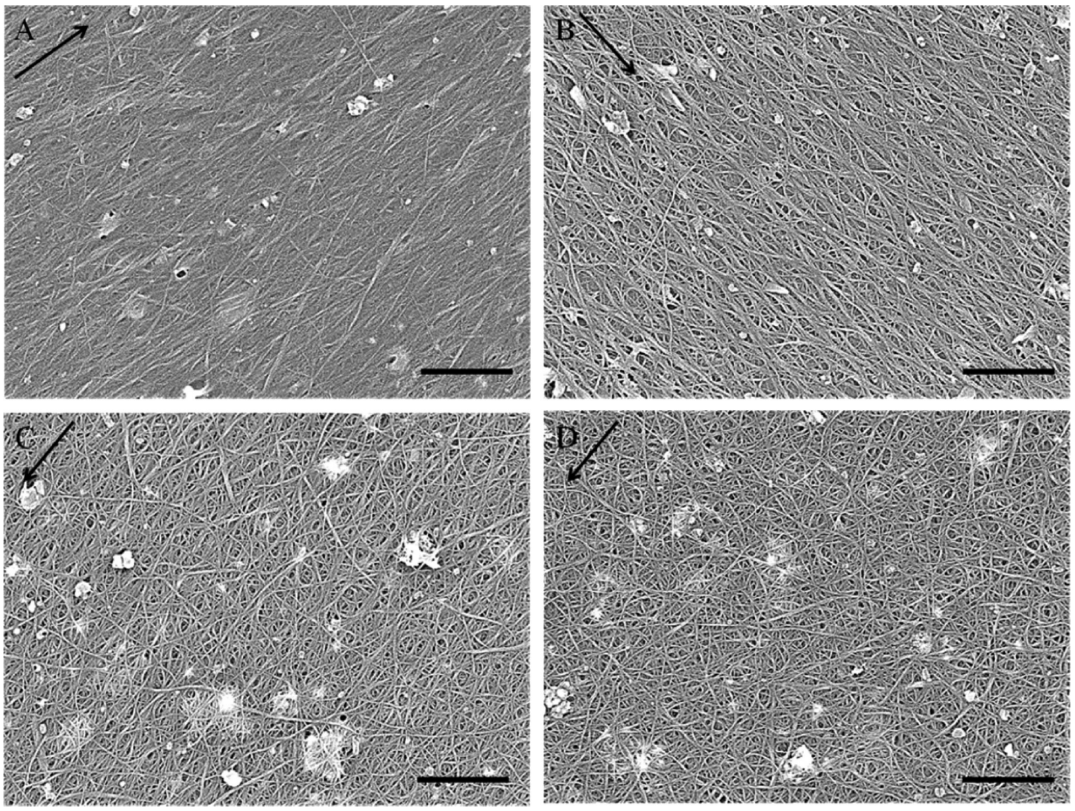

Figure 4. SEM images of SWNT/P3HT films at a 1:1 weight ratio cast at room temperature. (A) Highly aligned sample (pol. abs. ratio = 2.1) before polymer removal. B. Same highly aligned sample (pol. abs. ratio = 2.1) after polymer removal. (C, D). Two images of a moderately aligned sample (pol. abs. ratio = 1.2) after polymer removal. Local alignment is observed in each but different areas demonstrate different local orientations. Scale bars are 500 nm.

the alignment. Figure 5B shows a SEM image of a film made at 100 °C. There is an increased curvilinearity, which decreases alignment. In addition, the SWNT bundles are slightly larger at a diameter average of 22.5 nm. Larger bundles worsen transparent electrode performance.[52] This indicates that a flash evaporation is not desired for this type of deposition method because of the evaporative flow at higher temperatures.

Because the alignment is not sensitive to variations in shear rate for strong flows, it is not expected to be sensitive to various film applicator geometries, which slightly affect the shear rate and pressure gradient in the solution. Three applicator geometries were used and the alignment was monitored after the deposition. The three were a Mayer rod, which is a wire-wound bar; a Baker applicator, which is cylindrical; and a Bird applicator, which is wedge-shaped. A constant gap of 10 μm and shear rate of 10000 s^{-1} was used for this comparison. As shown in Figure 6A, the polarized absorbance ratio did not vary much across using these three applicators, ranging from 1.9 to 2.1. All films have similar characteristics as observed in SEM images B and C in Figure 6. The stress gradients induced by the different applicators will vary, such as the Baker applicator having a greater vertical component and the Mayer rod having both a greater lateral and vertical component, but these variations have not changed the alignment. Overall alignment did not change much regardless of how the dispersion is sheared.

To be a viable method for aligned SWNT films, the SWNT density must be controlled. High SWNT densities are preferred for most applications unless a mixture of metallic and semiconducting SWNTs is used for transistors. By varying the gap or the concentration, the density of the SWNT films varies. Figure 7 shows a dispersion cast at various gaps and concentrations. The two images show films with densities lower than presented in other SEM images. A gel-like dispersion was diluted after sonication by a factor of 10 to create the thinner film in Figure 7A. In this way, the gel-like properties, which enabled the alignment, were still maintained, though with weaker mechanical properties, as shown in the Supporting Information, Figure S1. The polarized absorbance ratio for the displayed film is 1.4. Figure 7B shows an image where the concentration was kept at 2 mg/mL but the gap was only 5 μm. Here the polarized absorbance ratio is 2.8. Though the densities in these films are decreased, the good alignment is still maintained. Combining both methods can yield lower density films. Low density, randomly oriented films can also be made by diluting the dispersion before sonication. An additional benefit is that the average SWNT bundle size decreased to 15 nm. Therefore, these films demonstrate that the SWNT density is tunable, from low, less than full coverage, to high density while still allowing for control of the alignment.

Comparing this alignment method with others is needed to test its feasibility. The ideal alignment method will have a significant control over alignment allowing for random to perfect orientations. Perfect alignment is needed when individual SWNTs span the device to maximize the current output while partial alignment is preferred for SWNT networks to improve the network connectivity.[16,17] In addition, this alignment must be unidirectional to allow for alignment of the device and network orientations. Density control is needed if the SWNT network contains both metallic and semiconducting

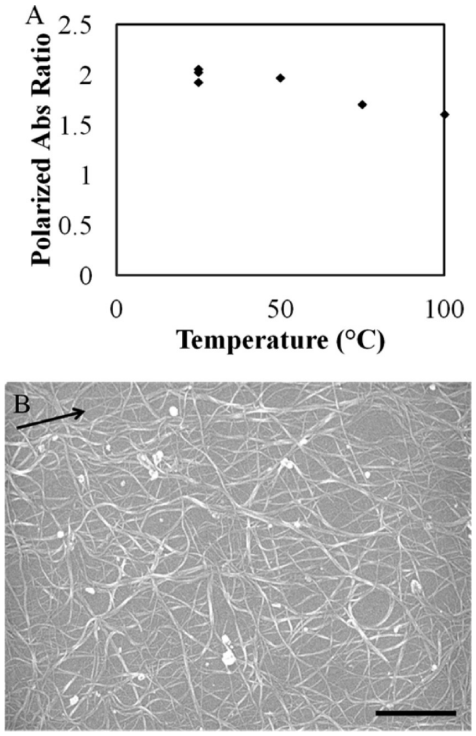

Figure 5. (A) Effect of substrate temperature. Polarized absorbance ratio for SWNT/P3HT films at a 2:1 weight ratio cast at a 10 000 s^{-1} shear rate as a function of substrate temperature. Values are given for absorption at 1000 nm. (B) SEM image of a film cast at 100 °C. Scale bar is 500 nm.

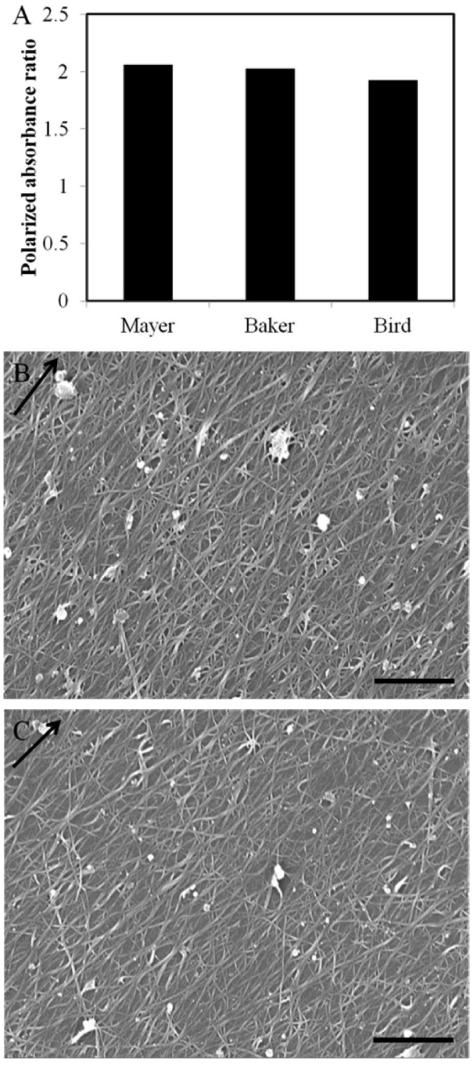

Figure 6. Effect of applicator used. (A) Comparison of alignment of films cast using three different film applicators for a 2:1 SWNT/P3HT dispersion. Values are given for absorption at 1000 nm. (B) SEM image of a film cast using a Mayer rod. (C) SEM image of a film cast using a Baker film applicator. Scale bars are 500 nm.

SWNTs. If the SWNTs are sufficiently sorted to have a high purity of metallic or semiconducting tubes, dense networks are preferred to give lower sheet resistances.[16] Low cost, substrate versatility, and scalability are also important factors to consider. One necessary parameter is that the alignment method must not hinder the performance of the SWNT network. Incorporation of insulating materials, such as surfactants for example, would hinder the electrical performance. Table 1 compares several methods using these guidelines. For example, the orientation of a SWNT network synthesized using the CVD method can be controlled from random to perfect alignment.[21,22] However, simultaneous density control has not been demonstrated. One advantage of CVD-deposited SWNTs is their good electrical performance. Long nanotubes can be grown with few defects, leading to high-quality films. However, the catalysts and amorphous carbon may still be in the film, which would hinder performance. Though using a quartz substrate to align nanotubes during CVD growth has many advantages, its scaling up over a large area is yet to be demonstrated. Additionally, the aligned SWNTs need to be subsequently transferred to the desired substrate, which adds additional costs to the process. High temperatures are needed for SWNT growth, typically above 600 °C[8] but usually around 900 °C.[20,23−25] In comparison, solution-processed films are typically coated in air and at room temperature. Nevertheless, the high performance of the CVD-aligned nanotubes would allow them to be used for more premier applications.

Solution-processed films can be made much more cheaply and faster than CVD-grown films. No high temperatures or other costly procedures are necessary but other unappealing characteristics can arise with solution processing. For example, the carbon nanotubes all have much shorter lengths because of the sonication and the limit of the length of SWNT that is dispensable, on the order of micrometers rather than hundreds of micrometers in CVD. In addition, one major difficulty with SWNT solutions is low solubility due to strong van der Waals interactions. One solution processing alignment method is to induce lyotropic liquid crystallinity by increasing the concentration of the SWNTs. This can be done by increasing the solubility of SWNT dispersions[39,40] or to take advantage of the concentration increase upon solvent evaporation.[41,42] The scalability and throughput would be areas of concern with slowly evaporating systems. Self-alignment is a promising method to align SWNTs on any substrate. For nanotubes forming liquid crystals, the nanotubes are already aligned domains in solution. This makes it is relatively easy to align these domains using very low stresses. Evaporation-driven self-alignment leads to well controlled systems. However, these processes could be limited to batch processes, which would lower the throughput for making devices. Table 1 summarizes this information as well as characteristics for other solution processing alignment methods.

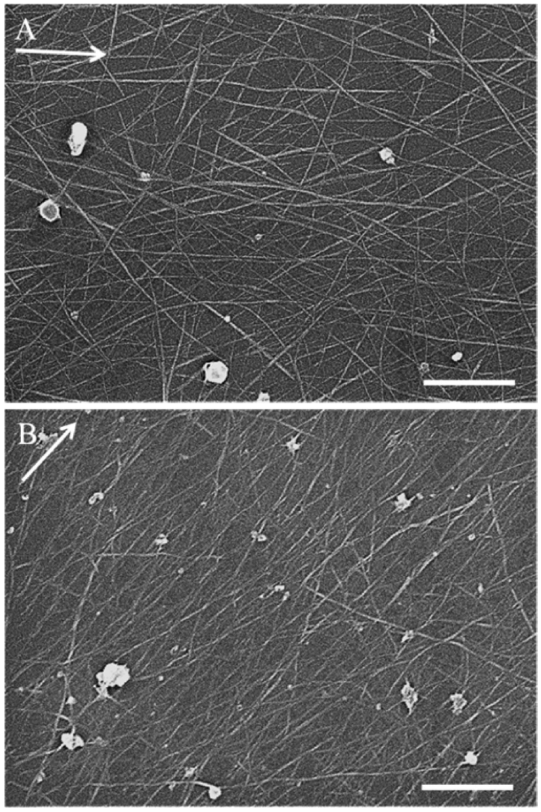

Figure 7. Controlling SWNT density by concentration and gap distance. SEM images of SWNT/P3HT (2:1) films with a decreased density. (A) Dispersion was diluted to 0.2 mg/mL after sonication. The polarized absorbance ratio is 1.4. (B) Dispersion at 2 mg/mL cast using a 5 μm gap. The polarized absorbance ratio is 2.8. Scale bars are 500 nm.

The alignment method introduced in this study involves weak gels with aligned domains. These gels are sheared at various speeds and with variable gaps to give a range of alignment and nanotube density. This method involves ultrasonication to disperse the SWNTs, but is limited to 15 min to minimize damage to the nanotubes. No centrifugation was necessary due to the good dispersion by P3HT and to have a better control over the concentrations and to simplify the process. This method allows alignment to be controlled from low levels of alignment to strong alignment. The cost of using this system would be very low compared to other methods. The disadvantage of using this alignment method is that the dispersant is a polymer. P3HT is more difficult to remove compared to surfactants. High temperatures, up to 500 °C, are needed to thoroughly remove it. In some applications, P3HT may not hinder performance because of its semiconductor properties.

To evaluate the effects of SWNT alignment on electrical behavior, the transparent electrode performance was used to correlate with the polarized absorbance ratio. Four-point probe sheet resistance and transmittance measurements were measured along different angles to the shearing direction. Some films cast from the nongel forming SWNT/regioregular poly (3-dodecyl thiophene) dispersions are included as films with random orientations for comparison.[45] Dropcast films of the SWNT/P3HT dispersion also lead to randomly oriented films. However, these films are very thick with a transmittance below 10%. Because of this, these films were not included in the correlation to more effectively probe only the effect of partial alignment. The percent transmittances for the films used in this study were all between 70 and 90% transparent. To combine the sheet resistance and transmittance into one figure of merit, the DC conductivity to optical conductivity ratio (D/O), a factor typically used to characterize the performance of transparent electrodes,[3,53−55] is used. It is defined as

$$\frac{\sigma_{DC}}{\sigma_{optical}} = \left(\frac{\sqrt{\frac{100}{\%T} - 1}}{188.5} R_s \right)^{-1}$$

where σ_{DC} is the electrical conductivity, $\sigma_{optical}$ is the optical conductivity, T is the transmittance, and R_S is the sheet resistance. Note that the conductivity of these films could be increased by various doping methods.[56] We did not do that since our main aim is to study the correlation between alignment and transparent electrode performance rather than maximizing the electrical performance. Nonetheless, D/O values of up to 11 have been reached using this method without doping. The details of the processing conditions are in the Supporting Information. The results of the correlation measurements are shown in Figure 8. The range of polarization ratios is from 0.5 to 2.2. As a comparison, in their SWNT alignment-transistor paper made from CVD growth, Kocabas et al. used an alignment standard of $L_{\parallel}/L_{\perp}$, which is proportional to the absorbance ratio. Their range was 3 to 21.[25] Thus, this correlation does not cover larger anisotropy ratios alignments that are achievable via CVD.

Nevertheless, a correlation between the alignment and the transparent electrode performance can be clearly seen. The rate of improvement in D/O per polarized absorbance ratio is about 1.2. The ratio of transparent electrode performance for films aligned best to the parallel to perpendicular directions is about 4.6. Simulations[16] have shown that the expected increase in performance between a randomly oriented film and a film with the ideal level of partial alignment is 1.5. However, it should be noted that these simulations used uniform individual single-walled carbon nanotubes with two-dimensional conduction rather than the nonuniform SWNT bundles with two-dimensional conduction used in this study. The transparent electrode performance depends on both the bundle length and diameter. Increasing the bundle length leads to improved electrical performance.[15] Increasing bundle diameter leads to more nanotubes that will absorb light without aiding the conductivity greatly, thus reducing transparent electrode performance.[52] No noticeable changes in bundle diameter or length were observed for any films used in forming the correlation. Thus, the comparison between this simulation and our work is applicable. Our rate of transparent electrode improvement with increasing SWNT alignment is greater than expected, indicating that these films are more sensitive to the SWNT orientation. If the level of alignment is further improved to be greater than that achieved in this study, as suggested in other studies,[25] films with a greater level of alignment may show an even greater increase in transparent electrode performance. This trend may continue with greater alignment up until the number of percolated pathways begins to drop.[17]

Films prepared from the same batch conditions were used so that we were able to remove external factors, such as changing SWNT density, film thickness, or SWNT bundle size, to make a connection between alignment and performance as a transparent electrode. This relates to how SWNT orientation affects

Table 1. Comparison of Various CNT Alignment Methods

	alignment method[a]	alignment control[b]	unidirectionality	CNT density control	CNT density range	substrate versatility	scalability	negative impact on performance	cost
CVD	vertically aligned forests[19,21]	random to perfect	yes	moderate	sub-monolayer to multiple layers	no	yes	no	high
	direct growth on quartz[20,22,23,25]	random to perfect	yes	moderate	sub-monolayer to 30/μm	no	yes	no	high
embedded in a matrix	liquid crystal[26−28]	low to nearly perfect	yes	good	sub-monolayer	yes	yes	yes	low
	confinement and compression[29]	random to nearly perfect	yes	good	submono-ayer to multiple layers	yes	no	yes	low
external forces	dielectrophoresis[30−34]	low to nearly perfect	yes	good	submonolayer to 30/μm	yes	no	no	low
	compression-sliding[35]	low to nearly perfect	yes	moderate	sub-monolayer to 80/μm	yes	yes	no	low
	gas flow[36,37]	random to strong	yes	poor	sub-monolayer	yes	no	no	low
	spin-coating[4,57,58]	low to strong	no	moderate	sub-monolayer to 45/μm	yes	no	no, enhanced[c]	low
	microfluidics[38]	low to strong	yes	good	sub-monolayer to 20/μm	yes	no	yes	low
	bubble blowing[59]	strong to nearly perfect	no	good	sub-monolayer	yes	no	yes	low
self-alignment	liquid crystallinity via superacids[39]	random to nearly perfect	yes	good	multiple layers	no	yes	yes	low
	liquid crystallinity via surfactants[40]	random to strong	yes	good	multiple layers	yes	yes	yes	low
	evaporation-driven[41,42]	random to strong	yes	good	5/μm to multiple layers	yes	yes	yes	low
	Langmuir−Blodgett[43]	random to strong	yes	good	monolayer up to 100/μm	yes[d]	no	yes[d]	low
	Langmuir−Schaefer[44]	random to strong	yes	good	monolayer up to 500/μm	yes[d]	no	yes[d]	low
this method	aligned, low yield stress gels	low to strong	yes	good	sub-monolayer to multiple layers	yes[d]	yes	yes[d]	low

[a]Transferred CNT networks are not considered here since all methods are amenable to transferring. [b]In terms of orientation order parameter, random, $S = 0$; low, $0 < S < 0.25$; strong, $0.5 < S < 0.75$; nearly perfect, $0.75 < S < 0.9$; perfect, $S \approx 1$. [c]Method also separates metallic and semiconducting nanotubes. [d]Depending on application because of the presence of conjugated polymers and the high temperatures required to remove them.

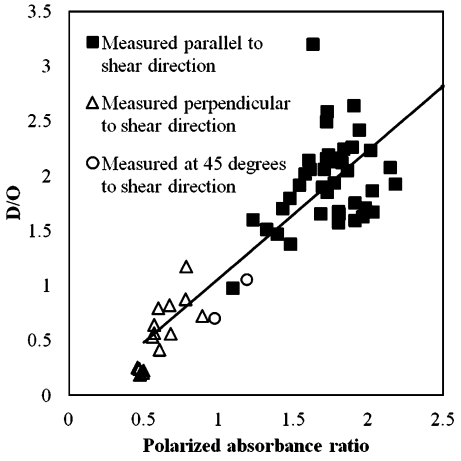

Figure 8. DC conductivity to optical conductivity ratios for SWNT/rrP3AT films at a 1:1 ratio as a function of the polarized absorbance ratio at 1000 nm. Resistance measurement were measured either parallel, perpendicular, or at a 45° angle to the shearing direction. A correlation between transparent electrode performance and SWNT alignment can be observed.

the resistance in a film. Simulations have been done previously but this work provides clear experimental findings proving the benefits of aligning nanotubes in a thin film. Though this deposition method limited the degree of alignment to a narrower range than past CVD studies, the SWNT density was kept consistent. We believe that aligning SWNTs will be a key factor in improving their transparent electrode performance in the future.

CONCLUSIONS

A simple and scalable SWNT alignment method has been presented. SWNTs wrapped with P3HT can form aligned gels in organic solvents. The aligned domains can be uniformly aligned with a modest shearing force. Due to their gel-like properties, the alignment is maintained as the solvent is evaporated. The resulting films have dense, unidirectional, partially aligned SWNTs. By modifying the deposition parameters, the level of alignment as well as the SWNT density can be controlled. Compared to other alignment methods, this is a promising one because of its ease of sample preparation. However, the presence of P3HT could be a problem for certain applications. The P3HT can be removed via calcination at 500 °C but this may limit the substrate versatility.

Using this aligned gel method, a correlation has been shown between alignment and transparent electrode performance over a range of partial alignments. Such a connection has not been shown experimentally and has not been thoroughly studied in simulations. Compared to the simulations that have been done,[16] our observed performance improvement was greater

than what has been predicted. We believe that this information will help the transparent electrode field as maximum ratios of DC to optical conductivities are pursued.

■ ASSOCIATED CONTENT

Supporting Information

A video demonstrating the evaporation of a drop of a SWNT/P3HT dispersion in 1,2-dichlorobenzene between crossed polarizers. The effect of diluting the dispersion after sonication on the rheological properties is also shown. Optimizing the processing conditions to maximize the transparent electrode performance is also presented. This material is available free of charge via the Internet at http://pubs.acs.org.

■ AUTHOR INFORMATION

Corresponding Author

*E-mail: ggf@stanford.edu (G.G.F.); zbao@stanford.edu (Z.B.).

Notes

The authors declare no competing financial interest.

■ ACKNOWLEDGMENTS

We thank the Center for Advanced Molecular Photovoltaics (CAMP) and Global Climate and Energy Project (GCEP) at Stanford University, and the Stanford Graduate Fellowship for funding this project.

■ ABBREVIATIONS

CNT, carbon nanotube
CVD, chemical vapor deposition
oDCB, 1, 2 dichlorobenzene
P3HT, regioregular poly (3-hexyl thiophene)
pol. abs, polarized absorbance
SEM, scanning electron microscope
SWNT, single-walled carbon nanotube

■ REFERENCES

(1) Han, J. In *Carbon Nanotubes: Science and Applications*; Meyyappan, M., Ed.; CRC Press: Boca Raton, FL, 2005; pp 1−30.
(2) Hu, L.; Hecht, D. S.; Grüner, G. *Chem. Rev.* **2010**, *110*, 5790−5844.
(3) Kumar, A.; Zhou, C. *ACS Nano* **2010**, *4*, 11−14.
(4) LeMieux, M. C.; Roberts, M.; Barman, S.; Jin, Y. W.; Kim, J. M.; Bao, Z. *Science* **2008**, *321*, 101−104.
(5) Chandra, B.; Afzali, A.; Khare, N.; El-Ashry, M. M.; Tulevski, G. S. *Chem. Mater.* **2010**, *22*, 5179−5183.
(6) Baughman, R. H.; Zakhidov, A. A.; de Heer, W. A. *Science* **2002**, *297*, 787−792.
(7) Dalton, A. B.; Collins, S.; Munoz, E.; Razal, J. M.; Ebron, V. H.; Ferraris, J. P.; Coleman, J. N.; Kim, B. G.; Baughman, R. H. *Nature* **2003**, *423*, 703−703.
(8) Dai, H. *Surf. Sci.* **2002**, *500*, 218−241.
(9) Li, W. Z.; Xie, S. S.; Qian, L. X.; Chang, B. H.; Zou, B. S.; Zhou, W. Y.; Zhao, R. A.; Wang, G. *Science* **1996**, *274*, 1701−1703.
(10) Lin, Y.; Taylor, S.; Li, H.; Fernando, K. A. S.; Qu, L.; Wang, W.; Gu, L.; Zhou, B.; Sun, Y.-P. *J. Mater. Chem.* **2004**, *14*, 527−541.
(11) Cao, Q.; Rogers, J. A. *Adv. Mater.* **2009**, *21*, 29−53.
(12) Hellstrom, S. L.; Jin, R. Z.; Stoltenberg, R. M.; Bao, Z. *Adv. Mater.* **2010**, *22*, 4204−4208.
(13) Wang, X.; Jiang, Q.; Xu, W.; Cai, W.; Inoue, Y.; Zhu, Y. *Carbon* **2013**, *53*, 145−152.
(14) Simien, D.; Fagan, J. A.; Luo, W.; Douglas, J. F.; Migler, K.; Obrzut, J. *ACS Nano* **2008**, *2*, 1879−1884.
(15) Hecht, D.; Hu, L.; Gruner, G. *Appl. Phys. Lett.* **2006**, *89*, 133112−3.
(16) Behnam, A.; Guo, J.; Ural, A. *J. Appl. Phys.* **2007**, *102*, 044313−7.
(17) White, S. I.; DiDonna, B. A.; Mu, M.; Lubensky, T. C.; Winey, K. I. *Phys. Rev. B* **2009**, *79*, 024301.
(18) Druzhinina, T.; Hoeppener, S.; Schubert, U. S. *Adv. Mater.* **2011**, *23*, 953−970.
(19) Pint, C. L.; Xu, Y.-Q.; Moghazy, S.; Cherukuri, T.; Alvarez, N. T.; Haroz, E. H.; Mahzooni, S.; Doorn, S. K.; Kono, J.; Pasquali, M.; Hauge, R. H. *ACS Nano* **2010**, *4*, 1131−1145.
(20) Kang, S. J.; Kocabas, C.; Ozel, T.; Shim, M.; Pimparkar, N.; Alam, M. A.; Rotkin, S. V.; Rogers, J. A. *Nat. Nanotechnol.* **2007**, *2*, 230−236.
(21) Xu, M.; Futaba, D. N.; Yumura, M.; Hata, K. *ACS Nano* **2012**, *6*, 5837−5844.
(22) Cao, Q.; Rogers, J. *Nano Res.* **2008**, *1*, 259−272.
(23) Wang, C.; Ryu, K.; De Arco, L.; Badmaev, A.; Zhang, J.; Lin, X.; Che, Y.; Zhou, C. *Nano Res* **2010**, *3*, 831−842.
(24) Orofeo, C. M.; Ago, H.; Ikuta, T.; Takahasi, K.; Tsuji, M. *Nanoscale* **2010**, *2*, 1708−1714.
(25) Kocabas, C.; Pimparkar, N.; Yesilyurt, O.; Kang, S. J.; Alam, M. A.; Rogers, J. A. *Nano Lett* **2007**, *7*, 1195−1202.
(26) Okano, K.; Noguchi, I.; Yamashita, T. *Macromolecules* **2010**, *43*, 5496−5499.
(27) Zhao, Y.; Xiao, Y.; Yang, S.; Xu, J.; Yang, W.; Li, M.; Wang, D.; Zhou, Y. *J Phys Chem C* **2012**, *116*, 16694−16699.
(28) Dierking, I.; Scalia, G.; Morales, P. *J. Appl. Phys.* **2005**, *97*, 044309−5.
(29) Islam, M. F.; Alsayed, A. M.; Dogic, Z.; Zhang, J.; Lubensky, T. C.; Yodh, A. G. *Phys. Rev. Lett.* **2004**, *92*, 088303.
(30) Fujitsuka, Y.; Oya, T. *J. Nanotechnol.* **2012**, *2012*, 5.
(31) Shekhar, S.; Stokes, P.; Khondaker, S. I. *ACS Nano* **2011**, *5*, 1739−1746.
(32) Yamamoto, K.; Akita, S.; Nakayama, Y. *J. Phys. D.: Appl. Phys.* **1998**, *31*, L34−L36.
(33) Senthil Kumar, M.; Lee, S. H.; Kim, T. Y.; Kim, T. H.; Song, S. M.; Yang, J. W.; Nahm, K. S.; Suh, E. K. *Solid-State Electron.* **2003**, *47*, 2075−2080.
(34) Chen, X. Q.; Saito, T.; Yamada, H.; Matsushige, K. *Appl. Phys. Lett.* **2001**, *78*, 3714−3716.
(35) Najeeb, C. K.; Chang, J.; Lee, J.-H.; Kim, J.-H. *Scr. Mater.* **2011**, *64*, 126−129.
(36) Hedberg, J.; Dong, L.; Jiao, J. *Appl. Phys. Lett.* **2005**, *86*, 143111−3.
(37) Xin, H.; Woolley, A. T. *Nano Lett* **2004**, *4*, 1481−1484.
(38) Park, J.-U.; Meitl, M. A.; Hur, S.-H.; Usrey, M. L.; Strano, M. S.; Kenis, P. J. A.; Rogers, J. A. *Angew. Chem.* **2006**, *118*, 595−599.
(39) Davis, V. A.; Ericson, L. M.; Parra-Vasquez, A. N. G.; Fan, H.; Wang, Y.; Prieto, V.; Longoria, J. A.; Ramesh, S.; Saini, R. K.; Kittrell, C.; Billups, W. E.; Adams, W. W.; Hauge, R. H.; Smalley, R. E.; Pasquali, M. *Macromolecules* **2003**, *37*, 154−160.
(40) Zamora-Ledezma, C.; Blanc, C.; Puech, N.; Maugey, M.; Zakri, C.; Anglaret, E.; Poulin, P. *Phys Rev E* **2011**, *84*, 062701.
(41) Huang, L.; Cui, X.; Dukovic, G.; O'Brien, S. P. *Nanotechnology* **2004**, *15*, 1450.
(42) Beyer, S. T.; Walus, K. *Langmuir* **2012**, *28*, 8753−8759.
(43) Li, X.; Zhang, L.; Wang, X.; Shimoyama, I.; Sun, X.; Seo, W.-S.; Dai, H. *J. Am. Chem. Soc.* **2007**, *129*, 4890−4891.
(44) Cao, Q.; Han, S.-j.; Tulevski, G. S.; Zhu, Y.; Lu, D. D.; Haensch, W. *Nat Nano* **2013**, *8*, 180−186.
(45) Allen, R.; Bao, Z.; Fuller, G. G. *Nanotechnology* **2013**, *24*, 015709.
(46) Lee, H. W.; You, W.; Barman, S.; Hellstrom, S.; LeMieux, M. C.; Oh, J. H.; Liu, S.; Fujiwara, T.; Wang, W. M.; Chen, B.; Jin, Y. W.; Kim, J. M.; Bao, Z. *Small* **2009**, *5*, 1019−1024.
(47) Lee, H. W.; Yoon, Y.; Park, S.; Oh, J. H.; Hong, S.; Liyanage, L. S.; Wang, H.; Morishita, S.; Patil, N.; Park, Y. J.; Park, J. J.; Spakowitz, A.; Galli, G.; Gygi, F.; Wong, P. H. S.; Tok, J. B. H.; Kim, J. M.; Bao, Z. *Nat. Commun.* **2011**, *2*, 541.

(48) Giulianini, M.; Waclawik, E. R.; Bell, J. M.; Scarselli, M.; Castrucci, P.; De Crescenzi, M.; Motta, N. *Appl. Phys. Lett.* **2009**, *95*, 143116−3.
(49) Pimparkar, N.; Kocabas, C.; Seong Jun, K.; Rogers, J.; Alam, M. A. *Electron Device Lett.* **2007**, *28*, 593−595.
(50) Ajiki, H.; Ando, T. *Physica B* **1994**, *201*, 349−352.
(51) Li, Z. M.; Tang, Z. K.; Liu, H. J.; Wang, N.; Chan, C. T.; Saito, R.; Okada, S.; Li, G. D.; Chen, J. S.; Nagasawa, N.; Tsuda, S. *Phys. Rev. Lett.* **2001**, *87*, 127401.
(52) Mustonen, K.; Susi, T.; Kaskela, A.; Laiho, P.; Tian, Y.; Nasibulin, A. G.; Kauppinen, E. I. *Beilstein J. Nanotechnol.* **2012**, *3*, 692−702.
(53) King, P. J.; Khan, U.; Lotya, M.; De, S.; Coleman, J. N. *ACS Nano* **2010**, *4*, 4238−4246.
(54) De, S.; Lyons, P. E.; Sorel, S.; Doherty, E. M.; King, P. J.; Blau, W. J.; Nirmalraj, P. N.; Boland, J. J.; Scardaci, V.; Joimel, J.; Coleman, J. N. *ACS Nano* **2009**, *3*, 714−720.
(55) De, S.; Higgins, T. M.; Lyons, P. E.; Doherty, E. M.; Nirmalraj, P. N.; Blau, W. J.; Boland, J. J.; Coleman, J. N. *ACS Nano* **2009**, *3*, 1767−1774.
(56) Duclaux, L. *Carbon* **2002**, *40*, 1751−1764.
(57) LeMieux, M. C.; Sok, S.; Roberts, M. E.; Opatkiewicz, J. P.; Liu, D.; Barman, S. N.; Patil, N.; Mitra, S.; Bao, Z. *ACS Nano* **2009**, *3*, 4089−4097.
(58) Wang, Y.; Pillai, S. K. R.; Chan-Park, M. B. *Small* **2013**, n/a−n/a.
(59) Yu, G.; Cao, A.; Lieber, C. M. *Nat. Nanotechnol.* **2007**, *2*, 372−377.